Journal of Engineering and Applied Sciences 14 (16): 5710-5718, 2019
ISSN: 1816-949X

Image Segmentation using Modified Region-Based Active Contour Model

Ooi Qun Wong and Parvathy Rajendran
School of Aerospace Engineering, Universiti Sains Malaysia, Engineering Campus,
14300 Nibong Tebal, Penang, Malaysia
aeparvathy@usm.my

Abstract: Image segmentation using active contour models to improve image processing enhances object detection. Various segmentation methods have been proposed over in the past to improve the accuracy of segmentation results such as clustering, edge-based, region-based, template matching and hybrid methods. However, the image segmentation results of these methods are not ideal. Therefore, a small improvement in the results will have a huge impact on image processing, particularly for autonomous unmanned aircraft application. Recently, the Chan-Vese Model, a region-based method that uses active contour models, gained considerable research attention because of its improved image segmentation capability. This study presents a model that enhances the Chan-Vese algorithm model. The main idea of the proposed method is to reduce the computational time in image segmentation without affecting the segmentation result. Fitting term is defined as constant in the proposed model and the level set equation of the main domain continues to evolve the curve toward the boundary of the object. A total of 467 images from the Berkeley segmentation database are used to test the proposed method and analyze its performance. Results indicate that the proposed model achieves better segmentation result with low computational time compared with existing image segmentation methods.

Key words: Object detection, segmentation, region-based method, active contour, fitting term, level set equation

INTRODUCTION

Image segmentation has been an active field of research for a long time because it is one of the main problems in image detection analysis for computer vision. The main objective of image segmentation is to segment an image into a few regions where image pixels do not overlap and have common characteristics with the ground truth. The majority of image processing work is applied to the computer vision field for visual tracking, object detection, pattern recognition (Yin *et al*., 2014), image colorization and contour detection (Arbelaez *et al*., 2011). Many previous research have studied image segmentation methods which can be classified into five classical techniques, namely, thresholding (Guo *et al*., 2014), clustering (Zhao *et al*., 2013, 2014; Krinidis and Chatzis, 2010; Zhao *et al*., 2015; He *et al*., 2012; Ji *et al*., 2012; Feng *et al*., 2013; Zhang *et al*., 2013), edge detection (Caselles *et al*., 1997), region growing (Chan and Vese, 2001) and template matching (Yoon *et al*., 2008).

Recent advanced technology has further improved and categorized these methods into supervised and unsupervised (Yang *et al*., 2013, 2014a, b), edge-based (Zhou *et al*., 2015) and region-based (Chan and Vese, 2001), soft-threshold (Pham and Prince, 1999) and hard-threshold (Pham, 2001) and parametric (Chan and Vese, 2001) and non-parametric (Joshi and Brady, 2010). Image thresholding methods are very effective and simple. However, traditional histogram-based thresholding algorithms cannot process the images of a target region that is much smaller than the background area (Gonzalez and Woods, 2009). The template matching method has a very simple working principle but it requires considerable work to derive the mathematical model.

A clustering method groups a set of multidimensional data into different similar data items together. This method is further divided into hierarchical and partitioning methods. Hierarchical method constructs clusters by partitioning the data in a way that splits large clusters or merges small clusters into large ones, respectively known as top-down and bottom-up partitioning.

Partitional clustering groups all the clusters into different groups at the initial partitioning and relocates one cluster into other clusters. The most common examples of partition clustering are k-Means (KM) (Duwairi and Abu-Rahmeh, 2015) and Fuzzy C-Means (FCM) clustering (Pham and Prince, 1999; Ji *et al*., 2012; Zhang *et al*., 2013; He *et al*., 2012; Wang *et al*., 2012; Krinidis and Chatzis, 2010; Feng *et al*., 2013; Ji *et al*., 2014). Wang *et al*. (2012) used FCM to extract the pixel-level feature of images and train the Support Vector Machine (SVM) (Haixiang *et al*., 2008) which acts as a

Corresponding Author: Parvathy Rajendran, School of Aerospace Engineering, Universiti Sains Malaysia, Enginnering Campus, 14300 Nibong Tebal, Penang, Malaysia, aeparvathy@usm.my

classifier to segment color images. This method used local information images for the input of the SVM Model such as the local spatial similarity measure model.

However, the local spatial information of an image will not produce good segmentation performance in images with noise (James, 1981). Hence, Zhao (2013) used non-local spatial information for fuzzy clustering algorithms with a filtering degree parameter which was applied differently for every pixel. Zhao *et al.* (2014) further improved the Suppressed Fuzzy C-Means clustering algorithms (S-FCM) by using self-tuning non-local filtering algorithms to overcome the weakness of S-FCM. Zhao's methods performed well with real images contaminated by noise (Zhao *et al*., 2014). Feng *et al.* (2013) also employed non-local FCM algorithms together with edge preservation to segment synthetic aperture radar images, a method that improved performance in terms of boundary localization and region uniformity.

Ji proposed a new method for generalized rough fuzzy C means (Ji *et al*., 2012) which is one of the hybrid clustering methods that combines fuzzy and rough sets and robust spatially constrained fuzzy C means (Ji *et al*., 2014). This method used a spatial factor to smooth and restore an image corrupted by noise, followed by a negative log posterior as a dissimilar function to classify the pixels for brain Magnetic Resonance Imaging (MRI) segmentation. Thus, Ji's method was robust to noise and initialization.

Hybrid method is also a very common approach for most researchers. Icer (2013) developed a hybrid method that fused Gaussian mixture modeling and FCM method for use in the medical field such as in segmenting real brain MRIs. This method is very useful in the medical field because it efficiently segments MRIs which are images constantly contaminated with noise.

Zhao *et al.* (2015) proposed another study on the Multi-objective Spatial Fuzzy Clustering Algorithm (MSFCA) which also, uses non-local spatial information as fitness functions. The group of final clusters was verified by a cluster validity index. This method performed well in grouping the number of clusters because it used a variable string length technique that transformed information in the cluster centers to algorithms. The advantage of MSFCA is that it can perform well on images with noises.

Meanwhile, Qin *et al.* (2014) proposed a new unsupervised method in image segmentation that combines the region saliency based on entropy rate superpixel with the affinity propagation clustering algorithm. Qin used the entropy rate superpixel method to divide the images into homogenous regions and convert them into saliency regions through the saliency estimation method (Frey and Dueck, 2007). Finally, Qin applied the affinity propagation clustering method (Frey and Dueck, 2007) to obtain the seed at a particular region in the image.

Unsupervised methods, also known as automatic approaches, do not require the user to participate in the segmentation process and have prior information related to the images. Hence, these interactive methods have received much attention in recent years because of their accuracy in segmentation result. Jung *et al.* (2014) adopted an unsupervised method that fused global k-means clustering and self-tuning spectral clustering. This fusion method was used initially to obtain the optimal initial seeds. The final segmented images were then obtained when the seed-kernel matrix was further propagated into the full-kernel matrix of the full image.

For the statistically based model, Dharmagunawardhana *et al.* (2014) proposed a method to improve texture description by using Gaussian Markov random fields. His method used local linear regression to determine the localized parameters and their distribution from the texture feature of the image. KM clustering algorithms were used together with texture descriptors to segment images for better segmentation results. Dharmagunawardhana's method showed better performance than the state-of-the-art texture descriptors. However, the boundary localization can be further improved using other methods such as hybrid method.

Wang *et al.* (2015) developed a new approach to color image segmentation by using the Pyramidal Dual-Tree Directional Filter Bank (PDTDFB) domain Hidden Markov Tree (HMT) statistical model. Gaussian mixture with HMT Model was used to model the PDTDFB coefficient. The Expectation-Maximization (EM) parameter estimation was used to define the parameters of the PDTDFB domain HMT Model. Wang *et al.* (2015) used Bayesian interscale fusion technique (Choi and Baraniuk, 2001) to ensure the finest scale was reached. Thus, the PDTDFB domain HMT statistical model can perform multidirectional transform and has high angular resolution.

Karadag and Vural (2014) proposed an unsupervised method that fused top-down and bottom-up segmentation maps under the Markov random field (Geman and Geman, 1984) framework. Karadag and Vural (2014) proposed a Mean Shift (MS) unsupervised method (Christoudias *et al*., 2002) to determine bottom-up segmentation maps and domain specific information and thus, construct top-down segmentation maps that contain general properties of the image dataset. Hence, the domain

specific maps were generated using the dataset and used together with the bottom-up segmentation maps to determine the energy function.

Region-based segmentation divides an image into regions and considers the gray level of the pixel within one region to have a similar value. Region-based techniques rely on the intensity values of one pixel and compare these with its neighbors. The pixel can be set to the region if the similarity criterion is satisfied. Generally, region-based image segmentation methods include region growing, Region Splitting (RS), Region Merging (RM) or their combinations in which all the connected pixels are grouped spatially into homogenous regions (Benz and Schreier, 2001).

Panagiotakis *et al.* (2011) proposed a general framework for image segmentation that uses feature extraction (Liapis *et al.*, 2004), classification in feature space (Matas and Kittler, 1995) and flooding and merging methods in spatial domain. The flooding algorithm, namely, priority multi-class flooding algorithm (Grinias, 2009), assigns pixels into labels of the image using Bayesian dissimilarity criteria (Sifakis *et al.*, 2002). The final step of this framework is the use of the RM method to obtain the final segmentation map on the basis of region features and edge localization (Canny, 1986).

MATERIALS AND METHODS

Active contour model: Generally, Active Contour Models (ACMs) (Kass *et al.*, 1988) find the contour to represent the boundary of objects in an image by minimizing an energy function (Mumford and Shah, 1989). ACMs use a level set framework (Osher and Fedkiw, 2003; Sethian, 1999) such as RM or RS, to make the contour change its topology (Sethian, 1999). ACMs are divided into edge-based and region-based models. One of the most popular region-based ACMs is the Chan-Vese (CV) Model (Chan and Vese, 2001) which uses curve evolution techniques (Caselles *et al.*, 1993), Mumford-Shah (MS) functional (Mumford and Shah, 1989) for segmentation and level set functions (Osher and Fedkiw, 2003) to determine the boundaries of objects without using the image gradient.

The C-V Model can segment images with object boundaries that are not well defined by the image gradient. Wang *et al.* (2014) conducted a research on a Region-Based Active Contour Model (RBACM) which combined local and global region fitting energies whose ratios could be adjusted by iterating the weighting coefficient for each iteration. The appropriate fitting energies were determined from the local and global Gaussian distributions with different variances and means. The weighting coefficient and time step were updated with the evolution of the contour to accelerate the convergence rate.

Meanwhile, Tran *et al.* (2014) improved the region-based method from the C-V Model (Chan and Vese, 2001) with the fuzzy energy-based active contour model by using a shape prior method to increase the speed and minimize the energy functional as well as employing a shape normalization procedure to properly align the image shapes. Ji *et al.* (2015) also proposed an RBACM that uses variational level set formulation and local Gaussian distributions. The energy minimization procedure used the means and variances of the local intensities to enable the local likelihood image fitting to propagate the initial curve toward the object boundaries. Nevertheless, the region-based method has a disadvantage in its performance when the images have severe intensity inhomogeneity.

The basic principle for edge-based methods is to evolve a curve to approach the boundaries of objects in an image whereas region-based methods partition an image into several homogeneous regions. The edge-based method detects the points because of the changes at the gray levels. Edge-based models use image gradients also known as edge information, to stop the evolving contours or surfaces on the object boundary. However, this method does not perform good segmentation on images with noise and is sensitive to contour initialization.

Caselles *et al.* (1997) proposed an edge-based method that uses curve evolution theory and image gradient as the edge detector function for boundary detection. Yang *et al.* (2014a, b) used the split Bregman (1967) method to solve the energy functional, improve the speed of computational time and globally convex the segmentation method into the piecewise constant multiphase as developed by the CV Model (Vese and Chan, 2002). Yang *et al.* (2014a, b) used an edge detector function to detect the boundaries of the images. Hence, Yang's method was more efficient than the CV Model (Vese and Chan, 2002). However, this edge-based technique does not work well when the images have many edges because the local image gradients attract contours toward the object boundaries.

Region-based method has more advantages than classical edge-based method mainly because the latter is easily confined into local minima. Meanwhile the former method is robust to noise, sensitive toward the initial curve and easily detects boundaries. Moreover, it utilizes the global image information (i.e., textures and colors) to detect weak boundaries. Although, all these methods are very successful in segmenting images in numerous applications, none of them can generally be applied to all

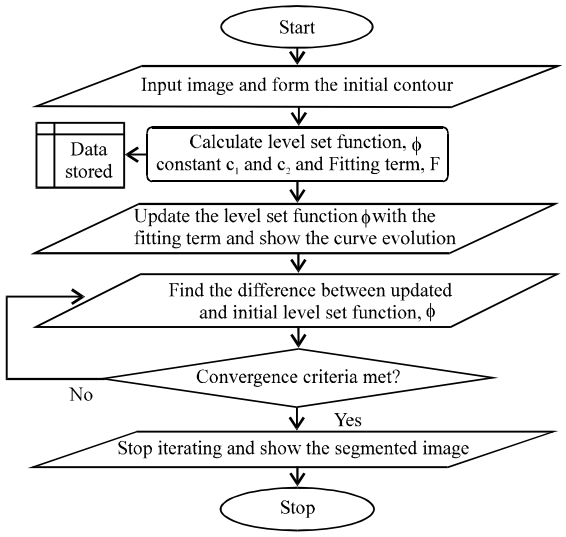

Fig. 1: Proposed algorithm flowchart

types of images such as synthetic, natural and real images. Thus, continuous improvements are required to ensure the accuracy of segmented images.

Proposed region-based ACM: The CV Model uses the curve evolution technique and level set method to determine the boundary of an object. The main concept in this model is the minimization of energy-based segmentation which uses local and global region information of the image to define the image fitting energy functional. This method uses fitting term and regularizing terms such as length of the curve and area of the region inside the curve, to form the energy functional equation, as shown in Eq. 1. where $\mu \geq 0$, $\nu \geq 0$, $\lambda_1 \geq 0$ and $\lambda_2 \geq 0$ are the constant parameters used. A summary of the proposed algorithm flowchart is shown in Fig. 1:

$$F(C, c_1, c_2) = \mu.\text{length}(C)+\nu.\text{area}(\text{inside}(C))+ \lambda_1\int_{\text{inside}(c)}|u_o(x, y)-c_1|^2+\lambda_2\int_{\text{outside}(c)}|u_o(x, y)-c_2|^2dxdy \quad (1)$$

In general, each term in the energy function equation is specifically defined. The first term is the length of the curve, the second term is the area inside the region, the third term is the fitting energy based on the inside region of the contour and the last term is the fitting energy term based on the outside region of the contour. These last two terms are the crucial parts that will affect the segmentation process of contour evolution if the value set is not in the correct range. Hence, the CV Model divides the image into two regions, namely, inside in (C) and outside out (C) regions. The level set formulation (Osher and Sethian, 1988) solves the energy minimization equation. The zero level set of the Lipschitz function ϕ is the boundary of the object. The energy equation is generally written in terms of the level set function as shown in Eq. 2:

$$\begin{aligned} F(c_1, c_2, \phi) = {} & \mu\int_\Omega \delta(\phi(x, y))|\nabla\phi(x, y)dxdy+ \\ & \nu\int_\Omega H(\phi(x, y))dxdy+\lambda_1\int_\Omega |u_o(x, y)- \\ & c_1|^2 H(\phi(x, y))dxdy+\lambda_2\int_\Omega |u_o(x, y)- \\ & c_1|^2 (1-H(\phi(x, y)))dxdy \end{aligned} \quad (2)$$

The first term in Eq. 2 is the length of the curve with the Dirac function. The second term is the area of the region inside the curve in terms of the Heaviside function. The last two terms which are the fitting terms also have the Heaviside function as shown in Eq. 3. The fitting terms with respect to the level set function are $c_1(\phi)$ and $c_2(\phi)$ functions as shown in Eq. 4 and 5, respectively. These constants are linked to the global properties of the region located inside and outside of the contour. The CV Model that adapts this method is weak in segmenting images with intensity inhomogeneity:

$$H(z(x)) = \frac{1}{2}\left(1+\frac{2}{\pi}\arctan\left(\frac{z}{\varepsilon}\right)\right) \quad (3)$$

$$c_1(\phi) = \frac{\int u_o(x, y)H(\phi(x, y))dxdy}{\int H(\phi(x))dxdy} \quad (4)$$

$$c_2(\phi) = \frac{\int u_o(x, y)(1-H(\phi(x, y)))dxdy}{\int (1-H(\phi(x)))dxdy} \quad (5)$$

Constant links to the global properties in relation to segmenting an image with intensity inhomogeneity will affect the accuracy of the segmentation result. Hence, the proposed model will fix the value of the constant in an acceptable range to improve the segmentation accuracy. This approach will eliminate the area of the region inside the curve and use the same value for the parameters of the fitting term inside and outside of the region, λ_1 and λ_2. To obtain the level set formulation, the energy functional is reduced to the level set function where, $c_1(\phi)$ and $c_2(\phi)$ are fixed. The Euler Lagrange equation is shown in Eq. 6:

$$\frac{\partial\phi}{\partial t} = \delta(\phi)\left[\mu\text{div}\left(\frac{\nabla\phi}{|\nabla\phi|}\right)-\nu-\lambda_1(u_o-c_1)^2+\lambda_2(u_o-c_2)^2\right] \quad (6)$$

The algorithm simulation will be initialized by reading the data of the images (i.e., pixels and bits information).

Then, a mask is required to create the initial contour which is also the initial level set function. The intensity of the image, inside and outside regions of the curve, image intensity and fitting term energy will be calculated. Later, the initial level set function is initialized and the program will start to optimize the level set function. The energy equation is then minimized until the convergence criterion is met. At this instance, the curve will start to evolve and the boundary of the object will be detected when the energy equation can no longer be minimized. The force optimization in the proposed algorithm is eliminated. Hence, the computational time is much lesser than that in the classical CV Model which needs to iterate the force energy equation.

Performance evaluation: Probabilistic Rand Index (PRI) Pantofaru and Hebert (2005) is the performance measure used to quantitatively evaluate and compare the efficiency of the proposed model. PRI counts the ratio of the labeled pixels that are consistent between the computed Segmentation, S_{test} and the ground truth Segmentation, S_k. In other words, it measures the percentage of compatibly classified pixel pairs in Segmentations of S_{test} and S_k as shown in Eq. 7:

$$PR\left(S_{test},\{S_k\}\right)=\frac{1}{\left(\frac{N}{2}\right)}\sum_{i<j}\left[c_{ij}p_{ij}+\left(1-c_{ij}\right)\left(1-p_{ij}\right)\right] \quad (7)$$

The value of PRI ranges from 0-1. The larger the value of PRI, the closer the segmentation result is to the ground truths and thus, the better the segmentation performance. This performance metric reliably measures the agreement between region-based segmented images and ground truth images, although, the two segments may have different numbers of regions (Foo *et al*., 2015).

RESULTS AND DISCUSSION

This study will present the segmentation results of the proposed model on real natural scene images for comparison, all these images were obtained from the Berkeley Segmentation Database (BSD500). The proposed algorithm was evaluated with the image size of 321×481 pixels. In our analysis, the proposed model involved five parameters established manually. In the level set function, the constants used were $\mu = 0.2$ for the signed distance function and $\nu = 0$ for the length of the contour. Moreover, $\lambda_1 = 1$ and $\lambda_2 = 1$ were equal for the inside and outside regions of the object.

The last parameter which is a very crucial factor to determine the accuracy of segmentation results was the time step value. The larger the time step, the faster the evolution of the curve an outcome that mathematically causes faster speed in the level set function equation. However, the boundary location of the image will be affected if the time step is too large. Hence, selecting a large time step can improve the computational speed but the trade-off will be the accuracy of the segmentation result in the boundary location. To obtain better segmentation results, time step $\nabla t = 0.5$ was used for all the simulations.

PRI performance: The proposed model was compared with the state-of-the-art segmentation approaches such as Finite Mixture Model (FMM) (Nguyen *et al*., 2013), Student's t Mixture Model (SMM) (Peel and McLachlan, 2000; Liu and Rubin, 1995), Spatially Variant Finite Mixture Model (SVFMM) (Blekas *et al*., 2005), robust Fuzzy Local Information C-Means (FLICM) (Krinidis and Chatzis, 2010) and Student's t Mixture Model with Spatial Constraints (SMM-SC) (Minh and Wu, 2012). For a fair comparison, the same images selected based on Nguyen *et al*. (2013) were evaluated to assess the performance of each model.

Table 1 shows the comparison of image segmentation PRI results on Berkeley's color image dataset for the five methods mentioned earlier together with the proposed model. Among 15 real world images, the proposed model performed well with the highest PRI value for most of the images.

Table 2 shows the average performance of the segmentation result given for all six methods listed in Table 1. Thus, the proposed model achieved the highest PRI average value of 0.752, outperforming other methods listed in the previous paragraph by at least 4.88% compared with FMM. The model also had the highest improvement of 9.14% compared with FLICM, followed by SMM at 6.81%.

Table 1: Comparison of PRI results on 15 images from the Berkeley database

Images ID	FMM	SMM	SVFMM	FLICM	SMM-SC	Proposed model
206062	**0.744**	0.731	0.742	0.714	0.743	0.7424
97010	**0.918**	0.877	0.913	0.845	0.915	0.7719
106005	**0.754**	0.735	0.748	0.719	0.748	0.7223
206097	0.692	0.687	0.690	0.689	0.690	**0.7013**
118015	**0.830**	0.785	0.826	0.799	0.828	0.7442
117025	**0.841**	0.834	0.837	0.816	0.841	0.6422
108069	0.505	0.501	0.502	0.502	0.505	**0.7932**
108036	0.678	0.668	0.673	0.662	0.674	**0.7608**
108004	0.627	0.617	0.616	0.604	0.626	**0.8782**
107072	0.705	0.701	0.705	0.668	0.704	**0.8134**
107045	0.630	0.619	0.624	0.605	0.626	**0.8397**
104055	**0.727**	0.723	0.725	0.713	0.727	0.6648
103029	0.624	0.621	0.621	0.620	0.625	**0.6492**
101027	**0.721**	0.719	0.720	0.676	0.721	0.7081
100039	0.756	0.746	0.750	0.708	0.754	**0.8474**

* Bold values are significant values

Table 2: Average PRI on 15 images from the Berkeley database

Methods	PRI	Percentage
FMM	0.717	4.88
SMM	0.704	6.82
SVFMM	0.712	5.61
FLICM	0.689	8.85
SMM-FC	0.715	5.17
Proposed method	0.752	-

Table 3: Average PRI of 90 images from the Berkeley database compared with KP and VOIBFM

Methods	PRI	Percentage
KP	0.7980	6.63
VOIBFM	0.8100	5.05
Proposed method	0.8509	-

Table 4: Comparison of iterations and CPU time (sec) between CV and proposed model

	Iteration number			CPU time (s)		
Images No.	CV Model	Proposed method	Percentage	CV Model	Proposed method	Percentage
124084	1083	883	**18.47**	55.69	23.83	**57.21**
296059	2769	995	**64.07**	134.78	18.64	**86.17**
135069	1549	1337	**13.69**	55.50	13.82	**75.14**
35070	919	866	**5.77**	38.39	13.77	**64.60**
12003	973	955	**1.85**	51.08	26.17	**48.77**
100075	904	882	**2.43**	50.14	26.00	**48.15**
56028	1282	1200	**6.40**	68.61	32.60	**52.49**
118020	948	840	**11.39**	50.78	22.15	**56.38**
8068	1129	258	**77.15**	40.66	23.88	**41.27**
3063	792	2572	**-224.74**	29.78	32.63	**-9.57**

*Bold values are significant values

Table 3 shows the average performance of the proposed method with Kernel Propagation (KP) method (Jung *et al*., 2014) and Variation of Information-Based Fusion Method (VOIBFM) to compare the segmentation results. The proposed method had the highest value of PRI at 0.8509 for 90 images. This result indicated that the proposed method performed better by at least 5.05% than the other two methods. The proposed method achieved better improvement than the KP method by 6.6%. In particular, the proposed method could be considered very efficient because the pair pixels of the segmentation were closer to the ground truths.

Computational time and iteration performance: The computational time of the proposed method with the region-based CV Model (Chan and Vese, 2001) on several natural images from Berkeley database images was analyzed. The computational time was based on the size of the initial contour that was set prior to running the simulation. Hence, the initial contour and parameters used for both methods were the same to ensure fair comparison. Both methods were implemented on an image size of 240×160 pixels using MATLAB and performed on a PC with Intel (R) Core (TM) CPU 1.80 GHz, 4 GB RAM. Table 4 displays the results of the 10 selected images based on the number of iterations and computational time (CPU).

The proposed method can reduce the computational cost for all the images. Hence, the proposed method is better than the CV Model in terms of computational cost. The proposed model achieved the highest improvement of 64.07% in iterations and 86.17% in computational time. However, among the 10 images compared, only one image had a slightly longer computational time by 3 sec.

The highest difference in computational time was approximately 120 sec for image ID of 296059. The proposed model improved by 86.17% of CPU time, in which the region-based active CV Model used 134.78 sec compared with the proposed method with only 18.64 sec. On average, the computational time for the proposed method was much faster than the CV Model by 59.5% and had 12.63% less iteration. Hence, the proposed model demonstrated a huge improvement in terms of computational cost in the long run.

CONCLUSION

The concept of region-based ACM was investigated in this study. The proposed method improved the CV Model (Chan and Vese, 2001) used in the force optimization technique to enhance the accuracy of the segmentation. The performance of the proposed model was compared with those of other segmentation methods in terms of quantitative evaluation and computational efficiency. The parameters set in the proposed method were applied to all types of images. Images were compared to visualize the segmentation accuracy of the proposed method and performance differences of the methods. The proposed model reduced half of the computational time, required fewer iterations and obtained better value of PRI compared with the CV Model. Hence, the proposed method achieved better performance in the quantitative evaluation and computational time. Thus, this algorithm may significantly improve real-time visual-based aircraft navigation.

ACKNOWLEDGEMENT

This research and publication was supported by Universiti Sains Malaysia Grant No. 304/PAERO/ 6031 5002.

NOMENCLATURE

C	: Curve
Length (C)	: Length of the Curve
Area (inside (C))	: Area inside the Curve
inside (C)	: Region inside the Curve
outside (C)	: Region outside the Curve
c_1	: Image intensity in the region inside the curve
c_2	: Image intensity in the region outside the curve
μ_0	: Gradient of the image
$\phi(x, y)$	: Level set function

H	:	Heaviside function
δ_0	:	One-dimensional dirac measure
$\delta(\phi)$	:	Dirac measure
div ($\nabla\phi/\|\nabla\phi\|$)	:	Divergence operator
μ	:	Constant parameter
ν	:	Constant parameter
λ_1	:	Constant parameter
λ_1	:	Constant parameter
N	:	Number of pixels in the image
c_{ij}	:	Number of pair of pixels and with the same label in image S_{test}
p_{ij}	:	Ground truth probability of two pixels with the same label estimated over all ground truth segmentations of the image

REFERENCES

Arbelaez, P., M. Maire, C. Fowlkes and J. Malik, 2011. Contour detection and hierarchical image segmentation. IEEE. Trans. Pattern Anal. Mach. Intell., 33: 898-916.

Benz, U. and G. Schreier, 2001. Definiens imaging GmbH: Object oriented classification and feature detection. IEEE. Geosci. Remote Sens. Soc. Newsl., 9: 16-20.

Blekas, K., A. Likas, N.P. Galatsanos and I.E. Lagaris, 2005. A spatially constrained mixture model for image segmentation. IEEE. Trans. Neural Networks, 16: 494-498.

Bregman, L.M., 1967. The relaxation method of finding the common point of convex sets and its application to the solution of problems in convex programming. USSR. Comput. Math. Math. Phys., 7: 200-217.

Canny, J., 1986. A computational approach to edge detection. IEEE Trans. Pattern Anal. Mach. Intell., 8: 679-698.

Caselles, V., F. Catt, T. Coll and F. Dibos, 1993. A geometric model for active contours in image processing. Numerische Math., 66: 1-31.

Caselles, V., R. Kimmel and G. Sapiro, 1997. Geodesic active contours. Int. J. Comput. Vision, 22: 61-79.

Chan, T.F. and L.A. Vese, 2001. Active contours without edges. IEEE Trans. Image Process., 10: 266-277.

Choi, H. and R.G. Baraniuk, 2001. Multiscale image segmentation using wavelet-domain hidden Markov models. IEEE. Trans. Image Process., 10: 1309-1321.

Christoudias, C.M., B. Georgescu and P. Meer, 2002. Synergism in low level vision. Proceedings of the International Conference on Object Recognition Supported by User Interaction for Service Robots, August 11-15, 2002, IEEE, Quebec City, Canada, ISBN:0-7695-1695-X, pp: 150-155.

Dharmagunawardhana, C., S. Mahmoodi, M. Bennett and M. Niranjan, 2014. Gaussian Markov random field based improved texture descriptor for image segmentation. Image Vision Comput., 32: 884-895.

Duwairi, R. and M. Abu-Rahmeh, 2015. A novel approach for initializing the spherical K-means clustering algorithm. Simul. Modell. Pract. Theor., 54: 49-63.

Feng, J., L.C. Jiao, X. Zhang, M. Gong and T. Sun, 2013. Robust non-local fuzzy C-means algorithm with edge preservation for SAR image segmentation. Signal Process., 93: 487-499.

Foo, Y.W., C. Goh, H.C. Lim, Z.H. Zhan and Y. Li, 2015. Evolutionary neural network based energy consumption forecast for cloud computing. Proceedings of the 2015 International Conference on Cloud Computing Research and Innovation (ICCCRI), October 26-27, 2015, IEEE, Singapore, ISBN:978-1-5090-0144-6, pp: 53-64.

Frey, B.J. and D. Dueck, 2007. Clustering by passing messages between data points. Science, 315: 972-976.

Geman, S. and D. Geman, 1984. Stochastic relaxation, Gibbs distributions and the bayesian restoration of images. IEEE. Trans. Pattern Anal. Mach. Intell., 6: 721-741.

Gonzalez, R.C. and R.E. Woods, 2009. Digital Image Processing. 3rd Edn., Pearson Education, London, England, UK., ISBN:978-81-317-2695-2, Pages: 977.

Grinias, E., 2009. Bayesian flooding for image and video segmentation. Ph.D Thesis, University of Crete, Rethymno, Crete.

Guo, Y., A. Sengur and J. Ye, 2014. A novel image thresholding algorithm based on neutrosophic similarity score. Meas., 58: 175-186.

Haixiang, X., C. Wanhua, C. Wei and G. Liyuan, 2008. Performance evaluation of SVM in image segmentation. Proceedings of the 2008 9th International Conference on Signal Processing, October 26-29, 2008, IEEE, Beijing, China, ISBN:978-1-4244-2178-7, pp: 1207-1210.

He, Y., M.Y. Hussaini, J. Maa, B. Shafei and G. Steidl, 2012. A new fuzzy C-means method with total variation regularization for segmentation of images with noisy and incomplete data. Pattern Recognit., 45: 3463-3471.

Icer, S., 2013. Automatic segmentation of corpus collasum using Gaussian mixture modeling and Fuzzy C means methods. Comput. Methods Programs Biomed., 112: 38-46.

James, C.B., 1981. Pattern Recognition with Fuzzy Objective Function Algorithms. Kluwer Academic Publishers, Berlin, Germany,.

Ji, Z., J. Liu, G. Cao, Q. Sun and Q. Chen, 2014. Robust spatially constrained fuzzy C-means algorithm for brain MR image segmentation. Pattern Recognit., 47: 2454-2466.

Ji, Z., Q. Sun, Y. Xia, Q. Chen and D. Xia *et al*., 2012. Generalized rough fuzzy c-means algorithm for brain MR image segmentation. Comput. Methods Programs Biomed., 108: 644-655.

Ji, Z., Y. Xia, Q. Sun, G. Cao and Q. Chen, 2015. Active contours driven by local likelihood image fitting energy for image segmentation. Inf. Sci., 301: 285-304.

Joshi, N. and M. Brady, 2010. Non-parametric mixture model based evolution of level sets and application to medical images. Intl. J. Comput. Vision, 88: 52-68.

Jung, C., J. Liu, T. Sun, L. Jiao and Y. Shen, 2014. Automatic image segmentation using constraint learning and propagation. Digital Signal Process., 24: 106-116.

Karadag, O.O. and F.T.Y. Vural, 2014. Image segmentation by fusion of low level and domain specific information via Markov Random Fields. Pattern Recognit. Lett., 46: 75-82.

Kass, M., A. Witkin and D. Terzopoulos, 1988. Snakes: Active contour models. Int. J. Comput. Vision, 1: 321-331.

Krinidis, S. and V. Chatzis, 2010. A robust fuzzy local information C-means clustering algorithm. IEEE Trans. Image Process., 19: 1328-1337.

Liapis, S., E. Sifakis and G. Tziritas, 2004. Colour and texture segmentation using wavelet frame analysis, deterministic relaxation and fast marching algorithms. J. Visual Commun. Image Represent., 15: 1-26.

Liu, C. and D.B. Rubin, 1995. ML estimation of the t distribution using EM and its extensions, ECM and ECME. Stat. Sin., 5: 19-39.

Matas, J. and J. Kittler, 1995. Spatial and feature space clustering: Applications in image analysis. Proceedings of the International Conference on Computer Analysis of Images and Patterns, September 6-8, 1995, Springer, Berlin, Germany, ISBN:978-3-540-60268-2, pp: 162-173.

Minh, N.T. and Q.M.J. Wu, 2012. Robust student's-t mixture model with spatial constraints and its application in medical image segmentation. Med. Imaging. Trans., 31: 103-116.

Mumford, D. and J. Shah, 1989. Optimal approximations by piecewise smooth functions and associated variational problems. Commun. Pure Applied Math., 42: 577-685.

Nguyen, T.M., Q.J. Wu, D. Mukherjee and H. Zhang, 2013. A finite mixture model for detail-preserving image segmentation. Signal Process., 93: 3171-3181.

Osher, S. and J.A. Sethian, 1988. Fronts propagating with curvature-dependent speed: Algorithms based on Hamilton-Jacobi formulations. J. Comput. Phys., 79: 12-49.

Osher, S. and R. Fedkiw, 2003. Level Set Methods and Dynamic Implicit Surfaces. 1st Edn., Springer, New York, USA., ISBN:978-0-387-95482-0, Pages: 273.

Panagiotakis, C., I. Grinias and G. Tziritas, 2011. Natural image segmentation based on tree equipartition, bayesian flooding and region merging. IEEE. Trans. Image Process., 20: 2276-2287.

Pantofaru, C. and M. Hebert, 2005. A comparison of image segmentation algorithms. Master Thesis, Carnegie Mellon University, Pittsburgh, Pennsylvania.

Peel, D. and G.J. McLachlan, 2000. Robust mixture modelling using the t distribution. Stat. Comput., 10: 339-348.

Pham, D.L. and J.L. Prince, 1999. An adaptive fuzzy C-means algorithm for image segmentation in the presence of intensity inhomogeneities. Pattern Recognit. Lett., 20: 57-68.

Pham, D.L., 2001. Spatial models for fuzzy clustering. Comput. Vision Image Understanding, 84: 285-297.

Qin, C., G. Zhang, Y. Zhou, W. Tao and Z. Cao, 2014. Integration of the saliency-based seed extraction and random walks for image segmentation. Neurocomputing, 129: 378-391.

Sethian, J.A., 1999. Level Set Methods and Fast Marching Methods: Evolving Interfaces in Computational Geometry, Fluid Mechanics, Computer Vision and Materials Science. 2nd Edn., Cambridge University Press, Cambridge, UK., Pages 378.

Sifakis, E., C. Garcia and G. Tziritas, 2002. Bayesian level sets for image segmentation. J. Visual Commun. Image Repr., 13: 44-64.

Tran, T.T., V.T. Pham and K.K. Shyu, 2014. Image segmentation using fuzzy energy-based active contour with shape prior. J. Visual Commun. Image Represent., 25: 1732-1745.

Vese, L.A. and T.F. Chan, 2002. A multiphase level set framework for image segmentation using the Mumford and Shah model. Int. J. Comput. Vision, 50: 271-293.

Wang, H., T.Z. Huang, Z. Xu and Y. Wang, 2014. An active contour model and its algorithms with local and global Gaussian distribution fitting energies. Inf. Sci., 263: 43-59.

Wang, X.Y., W.W. Sun, Z.F. Wu, H.Y. Yang and Q.Y. Wang, 2015. Color image segmentation using PDTDFB domain hidden Markov tree model. Appl. Soft Comput., 29: 138-152.

Wang, X.Y., X.J. Zhang, H.Y. Yang and J. Bu, 2012. A pixel-based color image segmentation using support vector machine and fuzzy C-means. Neural Networks, 33: 148-159.

Yang, Y., L. Guo, T. Wang, W. Tao and G. Shao *et al*., 2014a. Unsupervised multiphase color-texture image segmentation based on variational formulation and multilayer graph. Image Vision Comput., 32: 87-106.

Yang, Y., S. Han, T. Wang, W. Tao and X.C. Tai, 2013. Multilayer graph cuts based unsupervised color-texture image segmentation using multivariate mixed student's t-distribution and regional credibility merging. Pattern Recognit., 46: 1101-1124.

Yang, Y., Y. Zhao, B. Wu and H. Wang, 2014b. A fast multiphase image segmentation model for gray images. Comput. Math. Appl., 67: 1559-1581.

Yin, S., X. Zhao, W. Wang and M. Gong, 2014. Efficient multilevel image segmentation through fuzzy entropy maximization and graph cut optimization. Pattern Recognit., 47: 2894-2907.

Yoon, Y.G., S.L. Lee, C.W. Chung and S.H. Kim, 2008. An effective defect inspection system for polarized film images using image segmentation and template matching techniques. Comput. Ind. Eng., 55: 567-583.

Zhang, Y., W. Zhou, W. Xu and L. Li, 2013. Lymph node image segmentation based on Fuzzy C-means clustering and an improved chan-vese model. Proceedings of the 2013 6th International Congress on Image and Signal Processing (CISP), December 16-18, 2013, IEEE, Hangzhou, China, ISBN:978-1-4799-2764-7, pp: 621-625.

Zhao, F., 2013. Fuzzy clustering algorithms with self-tuning non-local spatial information for image segmentation. Neurocomputing, 106: 115-125.

Zhao, F., H. Liu and J. Fan, 2015. A multiobjective spatial fuzzy clustering algorithm for image segmentation. Appl. Soft Comput., 30: 48-57.

Zhao, F., J. Fan and H. Liu, 2014. Optimal-selection-based suppressed fuzzy C-means clustering algorithm with self-tuning non local spatial information for image segmentation. Expert Syst. Appl., 41: 4083-4093.

Zhao, F., L. Jiao and H. Liu, 2013. Kernel generalized fuzzy C-means clustering with spatial information for image segmentation. Digital Signal Process., 23: 184-199.

Zhou, Y., W.R. Shi, W. Chen, Y.L. Chen and Y. Li *et al*., 2015. Active contours driven by localizing region and edge-based intensity fitting energy with application to segmentation of the left ventricle in cardiac CT images. Neurocomputing, 156: 199-210.